Inorganic Chemistry

Article

pubs.acs.org/IC

# Role of Spin States in Nitric Oxide Binding to Cobalt(II) and Manganese(II) Porphyrins. Is Tighter Binding Always Stronger?

Mariusz Radoń*

Faculty of Chemistry, Jagiellonian University, Kraków, Poland

Supporting Information

**ABSTRACT:** Binding of nitric oxide (NO) to metalloporphyrins and heme groups is important in biochemistry while challenging to describe accurately by density functional theory (DFT) calculations. Here, the structural and thermochemical aspect of NO binding to Co(II) and Mn(II) porphyrins is investigated by DFT and DFT-D (dispersion-corrected) calculations, supported by reliable coupled-cluster methodology (CCSD(T)), and critically correlated with the experimental data. It is argued that whereas the bonding of NO to Co(II) porphyrin is a simple radical recombination, the bonding of NO to Mn(II) porphyrin is accompanied by a crossing of spin states. For this reason, the spin-state conversion energy contributes to the Mn−NO bond energy, and the paradigmatic correlation between bond length and bond energy is violated for the considered nitrosyl complexes: the Mn−NO bond is (structurally) shorter by ∼0.2 Å, albeit (energetically) weaker by a few kcal/mol, compared with the Co−NO bond. Moreover, none of the many tested DFT methods can reproduce the Co−NO and Mn−NO bond energies simultaneously, except for calculations with B3LYP*-D3, TPSSh-D3, and M06-D3 methods supplemented with the proposed spin-state energy correction (to compensate for an error on the calculated spin-state conversion energy). The results of this study are important to appreciate the role of spin-state changes in ligand binding properties of heme-related models. They also highlight the need for accurate calculations for correct interpretation of experimental data, including the qualitative structure−energy relationship.

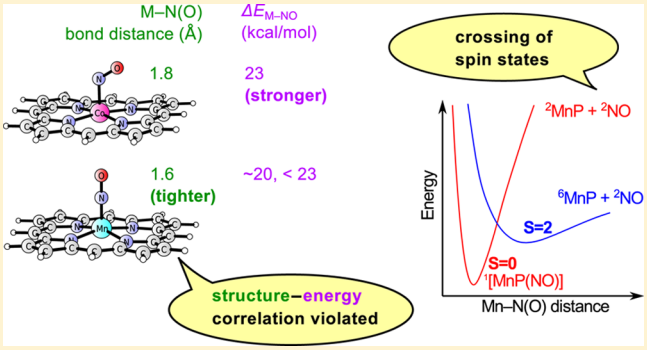


## INTRODUCTION

Binding of oxygen ($O_2$) and nitric oxide (NO) to metalloporphyrins and heme groups is of considerable biological importance: heme cofactors are well-known oxygen carriers (myoglobin, hemoglobin)[1] and signaling receptors of NO (soluble guanylate cyclase);[2] formation on an Fe−$O_2$ bond is also the first step of oxygen activation by P450 enzymes.[3] It is clear that for a detailed understanding of these enzymatic functions it is necessary to consider not only the metal cofactor but also the surrounding protein environment, taking into account secondary interactions with the distal groups and conformational changes caused by the ligand binding.[2,4] However, an affinity of the ligand toward the receptor is largely determined by its binding energy to the transition metal site, notwithstanding that it can be tuned by the protein environment.[5] Therefore, to describe the underlying metal−ligand bonding and electronic structure aspects relevant to ligand activation, a number of recent experimental[6−9] and computational[9−14] studies have been focused on the binding of $O_2$ and NO ligands (and CO as inhibitor) to isolated metalloporphyrin complexes. Such studies are preferably carried out in gas phase, in order to separate the intrinsic features of metal−ligand interaction from the effects of environment, such as solvent, counterions, or protein matrix.[6]

Although the process of ligand binding may seem simple and well understood from a computational perspective, it is not the case for the binding of noninnocent NO and $O_2$ ligands to open-shell transition metal sites. In fact, it is already a significant challenge to describe the complicated electronic structures of the resulting oxy- and nitrosyl-complexes, and to depict the metal−ligand bonding mechanism in strict chemical terms.[9,14−16] Another challenge for computational methods is to reproduce the metal−ligand bond dissociation energy with chemical accuracy.[11,12,17] In this regard, the recent studies of NO binding to Fe(II) and Fe(III) porphyrins revealed significant errors of common density functional theory (DFT) methods, some of which (hybrid functionals) tend to underestimate while others (pure functionals) tend to overestimate the Fe−NO bond energies.[11,12,18] This does not preclude the usefulness of DFT methods in computational bioinorganic chemistry, but it is vital to understand the origin of these large discrepancies because they may result in an incorrect description of ligand affinities toward the metalloprotein sites in studies of reaction mechanisms, and errors of this kind are unlikely to be compensated for by an elaborate

Received: December 29, 2014
Published: May 22, 2015





DOI: 10.1021/ic503109a
Inorg. Chem. 2015, 54, 5634−5645

treatment of the protein environment. The mentioned errors of DFT methods in metal−NO bond energies have been attributed to deficient treatment of nondynamical correlation effects[12] and dispersion (van der Waals) interactions[17] by approximate exchange-correlation functionals. Hence, the ability to correctly describe the metal−nitrosyl bond energy is not only important for the biological context but also may be regarded as a challenging accuracy test for DFT methods if they are meant to be used for related bioinorganic problems.

This Article is focused on the particularly interesting case of NO binding to Co(II) and Mn(II) porphyrins. The resulting nitrosyl complexes are analogues of iron heme groups with adsorbed $O_2$ and CO ligands, respectively, to which to they are isoelectronic, and they have been studied by various experimental methods. The enthalpy of homolytic Co−NO bond dissociation ($\Delta H_{Co-NO}$ = 23.4 kcal/mol) has been obtained for Co(TPP)(NO) (TPP = tetraphenylporphyrin) from titration calorimetry and suitable thermodynamic cycles.[19] Rather surprisingly, no precise experimental value is available for the analogous Mn−NO bond energy, although the MnNO porphyrin complexes can be isolated,[20,21] and the crystal structure of Mn(TPP)(NO) has been determined.[22] Nonetheless, Kubiak et al.,[21] have demonstrated by IR spectroscopy that the following nitrosyl transfer reaction occurs spontaneously by mixing the reactants:

$$\mathrm{Mn(TPP)(NO)} + \mathrm{Co(TPP)} \rightarrow \mathrm{Mn(TPP)} + \mathrm{Co(TPP)(NO)} \quad (1)$$

Moreover, attempts to perform the reverse reaction were unsuccessful, suggesting that reaction 1 is driven by thermodynamics, i.e., its Gibbs free energy must be negative ($\Delta G_{migr} < 0$) to account for the experimental behavior. In other words, the experimental data indicate that NO binds more favorably (in energetic sense) to Co(II) than to the Mn(II) porphyrin site.

Paradoxically, in the recent DFT study by Jaworska and Lodowski, the reverse order of binding energies has been found, i.e., the Mn−NO bond energy was reported to be *larger* than the Co−NO one by as much as 5−13 kcal/mol, depending on the method applied.[23] This unexpected result, although contrary to the outcome of the nitrosyl transfer experiment from ref 21, was rationalized by the fact that the NO ligand is more tightly bound (in the structural sense) to the Mn than to the Co site.[23] Indeed, based on the crystal structures of Mn(TPP)(NO)[22] and Co(TPP)(NO)[24b] complexes, the Mn−N(O) distance is only ∼1.6 Å, whereas the corresponding Co−N(O) distance is ∼1.8 Å, and this considerable difference in bond distance is also well reproduced by the calculations.[23] However, the author of this contribution believes that such structural arguments should be put aside when judging thermochemical stabilities of these nitrosyl complexes. It will be shown here that the ground spin state changes upon the bonding of NO to the Mn site, which has important consequences for an interplay between the bond energy and the equilibrium bond distance. The analogous effect of multiple spin states on NO binding have been first described in the example of {FeNO}$^6$ complexes by Praneeth et al., who explained the surprisingly low binding constant of NO by the crossing of spin states along the reaction coordinate.[25] It will be shown in this Article that a similar effect takes place here too. Moreover, it will be discussed that, due to the change of spin state during the formation of the Mn−NO bond, there is a problem with accuracy of DFT methods for the description of the bond energy, whose thermochemical consequences should not be overlooked.

To demonstrate the above, the structural and energetic aspects of NO binding to Co(II) and Mn(II) porphyrins will be studied here with a number of DFT and DFT-D (dispersion-corrected) methods, and critically compared with the available experimental data. Thermochemical corrections will be rigorously applied to the calculated Gibbs free energies, and the computational protocol will be validated by estimating the effects of solvation on the NO binding energies (however, it will be shown that these effects are small and relatively unimportant for the interpretation of the experimental data). In order to approach chemical accuracy, estimates of the relevant Co−NO and Mn−NO bond energies will also be obtained from reliable coupled-cluster calculations at the CCSD(T) level. (The CCSD(T) method, though computationally expensive, is regarded as a high standard of accuracy for a variety of chemical problems, including transition metal/bioinorganic systems.[12,26,27]) The discussion will be focused on the change of spin state accompanying the formation of the Mn−NO bond and on an analysis of its thermochemical consequences. This will allow us to confirm that and explain why the Co−NO and Mn−NO bonds in the studied nitrosyl−metalloporphyrin complexes violate the paradigmatic relationship between bond distance and bond energy (which is expressed in the title question: is tighter binding always stronger?).

## COMPUTATIONAL DETAILS

**Molecular Models.** Most of DFT calculations were performed for models with an unsubstituted porphin ring (P), which is a well established approximation for the computational treatment of metalloporphyrin complexes.[10,25,28] However, a few comparative calculations were also carried out for models with the full tetraphenylporphyrin ring (TPP). Structures of P and TPP rings with coordinated metal (M = Co, Mn) are shown schematically in panel a of Figure 1; panel b shows the arrangement of the NO ligand

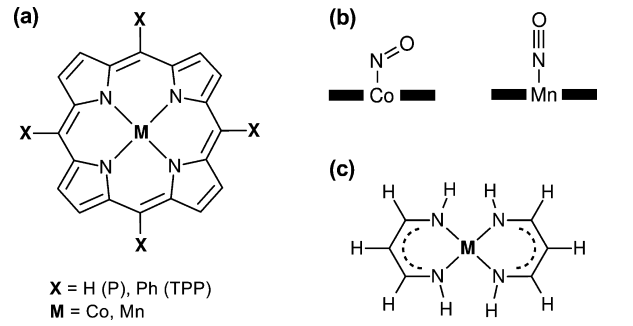


**Figure 1.** Structure of the metalloporphyrin unit with a porphin (P) or tetraphenylporphin (TPP) ring (a); orientation of the NO ligand above the ring plane (b); and structure of the $ML_2$ unit of simplified mimics (c).

above the macrocycle plane in the respective M−NO complexes. Optimized structures of nitrosyl complexes MP(NO) and their mimics $ML_2$(NO) can be found in Figure S1, Supporting Information.

The calculations to estimate the effect of ring approximation (P vs TPP) were performed only with selected DFT methods and the smaller basis set than the final set of calculations (for details and results, see Table S9, Supporting Information). It was found that the bond energies calculated for both types of models differ by at most 1 kcal/mol, and the difference of Co−NO and Mn−NO bond energies


DOI: 10.1021/ic503109a
Inorg. Chem. 2015, 54, 5634−5645

(the leading contribution to $\Delta G_{migr}$) calculated for both types of models agree to within 0.5−1.0 kcal/mol. The results thus confirm, in agreement with the literature,[25,28] that the use of an unsubstituted P ring is a very good approximation, whose effect on the calculated binding energies is much less pronounced than the dependence thereof on the choice of functional (see Results and Discussion).

CCSD(T) calculations of NO binding energies, due to their large computational cost, were carried out for simplified models (mimics), shown in Figure 1c, where two bidentate L ligands (L = $N_2C_3H_5^-$), arranged in one plane, serve to mimic the metal coordination by porphyrin. Similar mimics have been used in previous studies of heme-related models by different authors.[12,29,30] In order to maintain similarity with the P ring, structures of the mimics were optimized with added necessary constraints (symmetry or frozen dihedral angle) to keep coplanar the two L ligands.[30] Note that NO binding energies calculated for the mimics are clearly different from those for the corresponding porphyrin complexes, but an extrapolation procedure can be applied to obtain CCSD(T) estimates for the latter complexes (see below).

**DFT and DFT-D Calculations.** DFT and DFT-D (dispersion-corrected[31]) calculations were carried out with the Gaussian[32] and Turbomole[33] packages, employing a number of *pure* functionals, BP86,[34] OLYP[35] M06L,[36a] and B97-D;[31c] and *hybrid* functionals, PBE0,[37] B3LYP,[38] B3LYP*,[39] TPSSh,[40] and M06.[36b] Note that B97-D has already been constructed with dispersion correction included.[31c] For other DFT methods, the dispersion corrections were added using the most recent DFT-D3 approach of Grimme et al.,[31b] except for OLYP where the correction is not available. Since the DFT-D3 correction has not been explicitly parametrized for B3LYP*, the standard B3LYP parameters were used.

Unless indicated otherwise, molecular structures were optimized for each method with the def2-TZVP basis set, followed by single-point energy calculations with a larger basis set def2-Q(T), composed of def2-QZVPP for Co, Mn, N, and O; and def2-TZVPP for C and H. The computed bond energies were corrected for basis set superposition error (BSSE). Unscaled BP86/def2-TZVP harmonic frequencies were used to provide zero-point energy (ZPE) corrections to the bond energies and thermodynamical correction to the $\Delta G_{migr}$ values. The latter corrections were computed at $T$ = 298 K, $p$ = 1 atm using standard approximations (ideal-gas for translations, rigid rotations, and harmonic oscillations) as implemented in Turbomole. A correction for scalar relativistic effects was also included. Like in ref 30, it was obtained as the difference of second-order Douglas-Kroll (DK)[41] and nonrelativistic binding energies, calculated with the B3LYP* functional and cc-pVTZ-DK and cc-pVTZ basis sets, respectively. The applied corrections (BSSE, vibrational, relativistic) can be found in Tables S3−S5, Supporting Information. Note that, in agreement with the literature,[11,18] these corrections are much less sensitive to the applied DFT method than the electronic energy differences.

DFT calculations for all species with nonsinglet ground state were spin-unrestricted. The ground state of CoP(NO) and MnP(NO) complexes is singlet, but it was attempted to obtain a broken-symmetry (BS) solution[42] by performing spin-unrestricted calculations with an appropriate initial guess (i.e., after switching occupied/virtual 3d ± $\pi^*_{NO}$ orbitals in the $\beta$ set or providing BS orbitals converged with another functional). The BS solution was obtained only for hybrid functionals and their DFT-D3 counterparts: all of them in the case of CoP(NO) but only B3LYP(-D3) and PBE0(-D3) in the case of MnP(NO). For other methods, in particular all nonhybrid functionals (BP86, M06L, their -D3 counterparts, OLYP, and B97-D), it was possible to obtain a spin-restricted (SR) solution only, whose stability has been confirmed by positive eigenvalues of the electronic Hessian.[43] Analogous BS solutions were identified also for small mimics of the nitrosyl complexes. For all DFT methods leading to the BS description of the ground state, the BS solution was lower in energy than the SR solution, and thus, the BS solution was used in all further calculations presented in this work unless indicated otherwise (e.g., Supporting Information contains some SR results for comparison). In order to provide accurate NO binding energies, the BS DFT energies were corrected for spin contamination using the approximate spin-projection method:[44,45]

$$E_{pure} = E_{BS} - \langle \hat{S}^2 \rangle_{BS} \cdot \frac{E_{HS} - E_{BS}}{\langle \hat{S}^2 \rangle_{HS} - \langle \hat{S}^2 \rangle_{BS}} \quad (2)$$

In eq 2, the subscript HS refers to the auxiliary, high-spin state obtained by uncoupling the weakly coupled electron pairs found in the BS solution, whose energy and $\langle \hat{S}^2 \rangle$ value were computed separately in the geometry of the BS state. Since the BS solution for Co−NO/Mn−NO complexes contains one/two pair(s) of weakly coupled electrons, the appropriate HS state is triplet/quintet, respectively. Energetic effects of spin correction, effect of switching from SR to spin-projected BS description, and other details are reported in Tables S6−S7, Supporting Information. The electronic structure of BS solutions is discussed below (see Figure 2 and accompanying text).

Potential energy curves in Figure 4 were obtained with Gaussian by performing a series of unrestricted B3LYP*/def2-SV(P) optimizations in which the M−NO distance was constrained to different values. The minimum energy crossing point (MECP)[46] between the singlet and triplet energy surfaces of MnP(NO) was also calculated at the DFT-D/def2-TZVP level using B3LYP-D3 and TPSSh-D3 methods using the method earlier employed by Harvey for a similar purpose.[46b] The MECP calculations were performed with homemade program MECPy[47] based on the energies and gradients computed online by Turbomole. Note that the energy curves and MECP structures were computed without relativistic, BSSE, and spin-contamination corrections since they serve here only for qualitative purposes, not for quantitative comparison with experimental data.

**Estimates of Solvation Effects.** Calculations to estimate implicit solvation effects on the M−NO bond energies were carried out at the DFT/def2-TZVP level using COSMO (conductor-like screening model),[48] as implemented in Turbomole, with the dielectric constant of 25.592, corresponding to the benzonitrile solvent (in which $\Delta H_{Co-NO}$ was determined in ref 19). Despite the considerable polarity of this solvent, the effect on the M−NO bond energies turned out not to exceed 0.5 kcal/mol (see Table S10, Supporting Information).

In addition, explicit solvation was investigated for dichloromethane ($CH_2Cl_2$) and the tetrahydrofuran (THF) solvents mentioned in ref 21. This was done in view of previous suggestions that coordination of solvent molecules to the metal centers may perturb an interpretation of the nitrosyl migration experiment (reaction 1), although no calculations to illustrate this (hypothetical) effect have been presented.[23] The optimized structures of adducts with the solvent molecule can be found in Figure S3, whereas the estimates of the solvent binding energies in Table S11, both in Supporting Information. For obtaining reasonable supramolecular structures, particularly with $CH_2Cl_2$, it is important that DFT-D3 methods were used. The calculated solvent binding energies are sizable, on the order of 10−20 kcal/mol, suggesting that $CH_2Cl_2$-adducts will be in equilibrium with unsolvated complexes, whereas more stable THF-adducts may be even predominant in solution.[49]

From the difference of solvent binding energies to free MP and the corresponding MP(NO) complex (M = Co, Mn), the effect of solvation on the M−NO bond energy can be estimated (cf Table S11, Supporting Information). It is remarkable that despite considerable solvent binding energies (see above), the effect of solvation on the M−NO bond energy turns out to be astonishingly small: only 0.6−2.3 kcal/mol. As might be expected, formation of the adduct with $CCl_2H_2$ or THF molecule *trans* to NO, reduces the M−NO bond energy in all cases. However, the relative effect for two metals (Co versus Mn) is different for each of the considered solvents. For $CCl_2H_2$, the solvation effect is larger for Mn−NO than for the Co−NO bond energy, albeit the difference is very small (only 0.3−0.6 kcal/mol, depending on functional). For THF, the effect is larger for Co−NO than for the Mn−NO bond energy, and the difference is somewhat larger (0.4−1.4 kcal/mol, depending on functional).

In sum, the differential effects of solvation turned out to be very small, typically not exceeding 1 kcal/mol. This is in line with a nonionic character of the discussed processes of ligand binding and


DOI: 10.1021/ic503109a
Inorg. Chem. 2015, 54, 5634−5645

Table 1. Selected Structural Parameters and Stretching Frequencies from DFT Calculations with Various Functionals and Experimental Data[a]

| | | M−N(O)[b] | N−O[b] | ∠MNO[c] | $\nu_{N-O}$[d] | $\nu_{M-NO}$[d] |
|---|---|---|---|---|---|---|
| CoP(NO) | BP86 | 1.810 | 1.174 | 123.0 | 1689 | 567 |
| | OLYP | 1.811 | 1.169 | 123.5 | 1721 | 558 |
| | B3LYP | 1.960 | 1.151 | 123.2 | 1849 | 430 |
| | B3LYP* | 1.871 | 1.158 | 122.6 | 1783 | 487 |
| | TPSSh | 1.848 | 1.161 | 122.5 | 1772 | 508 |
| | Exptl | 1.844[e] | 1.164[e] | 122.7[e] | 1677[e,i] | |
| | | 1.83[f] | 1.01[f] | 135.2[f] | 1689[f,i] | |
| | | 1.855[g] | 1.158[g] | 120.6[g] | 1684[j] | 517[k] |
| MnP(NO) | BP86 | 1.611 | 1.180 | 180 | 1780 | 724 |
| | OLYP | 1.601 | 1.177 | 180 | 1807 | 725 |
| | B3LYP | 1.612 | 1.164 | 180 | 1836 | 522 |
| | B3LYP* | 1.605 | 1.167 | 180 | 1828 | 742 |
| | TPSSh | 1.602 | 1.168 | 180 | 1835 | 749 |
| | Exptl | 1.641[h] | 1.160[h] | 177.8[h] | 1735[h,i] | |
| | | | | | 1750[j] | |
| | | | | | 1739[l] | |
| $[FeP(NO)]^-$ | BP86 | 1.776 | 1.203 | 125.4 | 1543 | 567 |
| $[FeP(NO)]^+$ | BP86 | 1.615 | 1.154 | 180 | 1902 | 690 |
| free NO | BP86 | | 1.158 | | 1884 | |

[a]Note that B3LYP (M = Co and Mn) as well as B3LYP* and TPSSh (M = Co) provide the BS description of the singlet ground state; other included DFT methods provide the SR description of the ground state. [b]Values in Å. [c]Value in degrees. [d]Values in $cm^{-1}$; note that stretching Co−NO and bending Co−N−O modes are mixed in the case of CoP(NO); the higher-frequency combination is taken here as $\nu_{Co-NO}$, like in ref9. [e]Co(OEP)(NO), ref24a. [f]Co(TPP)(NO), ref24b (note that this value may be less reliable due to structural disorder). [g]Co(TP(*p*-OMe)P)(NO), ref24c, d. [h]Mn(TPP)(NO), ref22. [i]IR in KBr pellet. [j]IR of Mn(TPP)(NO)/Co(TPP)(NO) in solution, ref21. [k]RR of Co(TMP)(NO) in $CH_2Cl_2$, ref9. [l]IR of amorphous Mn(TPP)(NO) from ref55, the band attributed to the singlet ground state.

justifies the neglect of solvation in the mainstream of calculations reported here. Even for the case of THF, which binds rather strongly to both metal sites, the effect on $\Delta G_{migr}$ does not exceed 1.5 kcal/mol. More importantly, this effect has the wrong sign to account for the major discrepancy of most of the DFT calculations with the experiment (see Results and Discussion); namely, it would make $\Delta G_{migr}$ even more positive than that in unsolvated calculations, whereas the experimental data suggest that $\Delta G_{migr} < 0$.

**Coupled-Cluster Calculations.** Coupled-cluster calculations at the CCSD(T) level were carried out with Molpro[50] on top of the DFT-optimized structures (BP86/def2-TZVP). The reference function was RHF (singlet) or ROHF (other spin states); in the latter case, the RCCSD(T) formulation[51] was employed. Since CCSD(T) calculations for full porphin models, MP(NO), are at present computationally too expensive, the calculations were instead performed for their simplified mimics, $ML_2(NO)$ (M = Co, Mn; see Molecular Models). On the basis of the latter calculations, the estimates of CCSD(T) energies for porphyrin complexes were obtained with the aid of the extrapolation procedure introduced in ref 30. It is based on the observation that DFT results obtained from different functionals for an $L_2$-mimic and the corresponding P-model typically remain in a very good linear correlation ($R > 0.99$).[30] Good linear correlation is observed here too, in regard to the M−NO bond energies (M = Co, Mn) computed for both models with 12 different DFT/DFT-D methods (see Figure S5, Supporting Information). On the basis of the fitted trend lines and the results of CCSD(T) calculations for the mimics, it is possible to obtain CCSD(T) estimates of M−NO bond energies for the corresponding porphyrin complexes (details can be found in Figure S5 and Table S12, Supporting Information). ZPE and thermal corrections to $\Delta G_{migr}$ were added to the resulting estimates, based on the DFT:BP86/def2-TZVP frequencies.

In order to provide CCSD(T) results close to the complete basis set (CBS) limit, a similar computational protocol was applied as in ref 30 (to which the reader is pointed for more details and justification). The relative energy at the CCSD(T) level is composed of three contributions, calculated independently:

$$\Delta E_{CCSD(T)} = \Delta E_{CCSD}^{(nrfc)} + \Delta \varepsilon_{CCSD}^{(rcc)} + \Delta E_{(T)}$$

where (1) $\Delta E_{CCSD}^{(nrfc)}$ is nonrelativistic, frozen-core energy at the CCSD level computed at the CCSD-F12b level;[52] (2) $\Delta \varepsilon_{CCSD}^{(rcc)}$ is a correction to the former term for relativity and metal outer-core (3s3p) correlation; and (3) $\Delta E_{(T)}$ is the contribution of connected triples (T) to the correlation energy. Note that explicitly correlated (F12) calculations[53] were performed for the $\Delta E_{CCSD}^{(nrfc)}$ term, whereas CBS extrapolation was used for the $\Delta \varepsilon_{CCSD}^{(rcc)}$ and $\Delta E_{(T)}$ terms. Detailed procedures can be found in Supporting Information (page S13). The relativistic effects were included up to the second-order DK level.[41]

## RESULTS AND DISCUSSION

**Geometry, Vibrational Frequencies, and Electronic Structure.** Before going to the main point of this article, that is to a discussion of NO binding energies, it is necessary to start from a brief analysis of geometry and electronic structure of the studied complexes. For more elaborate discussions of vibrational frequencies of CoP(NO) and structural parameters of both complexes, the reader is referred to the literature.[9,23]

Table 1 reports the key structural parameters (M−NO distance, N−O distance, and MNO angle) and wave numbers of selected stretching vibrations ($\nu_{N-O}$ and $\nu_{M-NO}$) relevant to the description of metal−NO bonding. Only results from selected DFT methods are included, but more can be found in Table S1, Supporting Information. The calculations are, overall, in good agreement with the available experimental data, correctly reproducing in particular (a) the binding mode of NO ligand: linear in MnNO versus bent in the CoNO complex; (b) a much shorter Mn−N(O) bond distance (∼1.6 Å) compared with the Co−N(O) one (∼1.8 Å).

The difference of ∼0.2 Å in the M−N(O) bond distance (shorter bond for Mn) is significant and becomes even more considerable when taking into account the fact that the covalent


DOI: 10.1021/ic503109a
Inorg. Chem. 2015, 54, 5634−5645

radius of Mn is *larger* by 0.1 Å than that of Co.[54] Moreover, the calculated $\nu_{Mn-NO}$ frequency is much larger than the corresponding $\nu_{Co-NO}$ one. This is in accord with the shorter Mn−N(O) distance and supports the notion of tighter NO binding to the Mn than to the Co site. The $\nu_{N-O}$ stretching frequencies are best reproduced by the pure functional BP86. Higher $\nu_{N-O}$ frequency is observed for Mn than for the Co complex, according to both the experimental data and calculations with nearly all tested functionals (B3LYP being an exception).

A purely structural analysis would point to traditional formulation of the studied complexes as $Co^{III}-NO^{-}$ (explaining the bent CoNO motif) and $Mn^{I}-NO^{+}$ (explaining the linear MnNO motif). However, measurable properties of the NO ligand, such as the $\nu_{N-O}$ frequency and the N−O distance, in these complexes do not follow their formal $NO^{-}/NO^{+}$ assignment. This is best seen by comparison with computational DFT:BP86 data of two iron complexes, $[FeP(NO)]^{-}$ and $[FeP(NO)]^{+}$, for which the $NO^{-}/NO^{+}$ character is appreciable[25,56] and evidenced by (a) a significant red-/blue-shift of $\nu_{N-O}$ and (b) elongation/shortening of the N−O distance, as compared with free NO (cf Table 1). However, for CoP(NO) and MnP(NO) complexes the analogous trends are much less clear. As might be expected, $\nu_{N-O}^{MnNO} > \nu_{N-O}^{CoNO}$, but unexpectedly, both $\nu_{N-O}$ frequencies are *lower* and both N−O distances are *longer* than those for free NO. More curiously, the N−O distance in MnP(NO), formally assigned as the $NO^{+}$ complex, is *slightly longer* than the analogous distance in CoP(NO), formally assigned as the $NO^{-}$ complex. This holds true at least according to DFT:BP86 calculations, whereas the crystal structure data are less conclusive (the mentioned difference in bond distance is small and thus easily affected by crystal packing effects), although they also indicate that the (Co)N−O distance is about the same as the (Mn)N−O one, if not slightly shorter. The mentioned effects should be attributed to the considerable covalency of the studied metal−nitrosyl bonds,[57] making *formal* oxidation states not reflecting *real* properties of the bound NO ligand. The covalency is emphasized by using Feltham−Enemark notation:[58] here $\{CoNO\}^{8}$ and $\{MnNO\}^{6}$.

A detailed description of the electronic structure of these nitrosyl complexes (in particular oxidation state assignment) is beyond the scope of this study. However, one must recall that some of DFT calculations with hybrid functionals point to a BS description of the singlet ground state, whereas for other methods only the SR solution can be obtained. As mentioned in Computational Details, the BS solution for CoP(NO) is obtained for all hybrid functionals, whereas for MnP(NO) it is obtained only for B3LYP and PBE0. Detailed characteristics of BS solutions ($\langle S^2 \rangle$ values, natural orbital occupation numbers, and measures of their energetic stability compared with the SR solutions) are provided in Tables S6−S7, Supporting Information.

The natural orbitals and spin density from a typical BS calculations for CoP(NO) are shown in Figure 2. The BS solution describes one pair of weakly coupled electrons in two active orbitals: the bonding and antibonding combination of Co $d_{z^2}$ and NO $\pi_x^*$ (cf. Figure 2a). A fractional occupation of the antibonding and equal depopulation of the bonding orbital ($n_b + n_a = 2$), reflect a certain biradical character in the ground state of CoP(NO) due to nondynamical correlation in the Co−NO bond. This also results in a polarized spin density, with an excess of $\alpha$-spin density on Co and an excess of $\beta$-spin density on NO, reminiscent of antiferromagnetically coupled $Co^{II}$ and

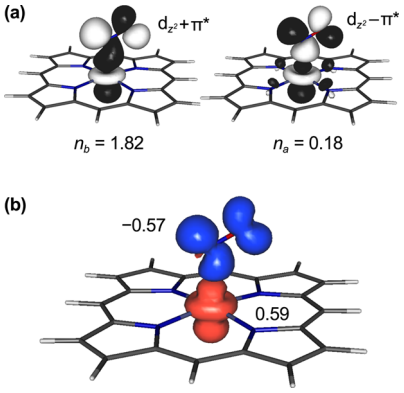


**Figure 2.** (a) Pair of natural orbitals with fractional occupation numbers (annotated) and (b) spin density with Mulliken spin populations of Co and NO, from BS B3LYP*/def2-TZVP calculations for CoP(NO). Isosurfaces ±0.04 (a) and 0.005 (b) a.u. Note that $n_a + n_b = 2$, and the $\langle S^2 \rangle_{BS}$ value is 0.345 ≈ $n_b n_a$, as expected of the BS DFT solution with one pair of active orbitals (cf. ref 59).

NO radicals (cf. Figure 2b). However, the fractional spin populations evidence that $Co^{II}-NO^{0}$ is merely one of the resonance structures contributing to quantum chemical description of the Co−NO bond (the other important ones are $Co^{III}-NO^{-}$ and presumably $Co^{I}-NO^{+}$). More advanced analysis of bonding in these complexes, based on multiconfigurational wave function,[15,60] is underway in our group and will be published in due course. The electronic structure of the Co−NO complex is thus partly analogous to oxy-heme porphyrin species, containing the isoelectronic Fe−$O_2$ core, whose biradical character reflects a contribution of antiferromagnetically coupled $Fe^{III}$ and $O_2^{-}$ radicals (i.e., the Weiss resonance structure).[14] However, the fractionally occupied natural orbitals are markedly different in these two cases, indicating a $\pi$-type radical coupling in the case of the Fe−$O_2$ bond (cf. ref 14) versus a $\sigma$-type coupling in the case of the Co−NO bond (cf. Figure 2). For MnP(NO), due to the linear geometry of the MnNO motif, there are two pairs of weakly coupled electrons in two pairs of symmetry-equivalent active orbitals of $d_{xz} \pm \pi_x^*$ and $d_{yz} \pm \pi_y^*$ character (see Figure S4, Supporting Information).

In agreement with the literature,[15,42,60−62] the existence of the BS solution as well as the amount of biradical character in it (related to spin contamination) are strongly dependent on the exchange−correlation functional, mainly on the exact exchange admixture. This is presumably related to the way different DFT methods deal with nondynamical (left−right) electron correlation in metal−nitrosyl bonding.[12,63] Pure functionals attempt to describe these correlation effects implicitly with the aid of the exchange-correlation functional; it is known that self-interaction error (SIE) in DFT can roughly simulate left−right correlation effects.[63,64] In turn, the admixture of exact exchange in hybrid functionals partially removes the SIE, while introducing a known tendency of HF (exact exchange) to breaking spin symmetry in order to account for nondynamical correlation. Moreover, even for pure functionals, which give SR solution near the equilibrium geometry, the BS solution appears when the M−NO bond is slightly elongated (e.g., for BP86 if the Co−NO distance is longer than ∼2.2 Å). The present author is thus far from treating the BS and SR solutions as two distinct electronic states. Both solutions should be rather viewed as approximations to the same singlet ground state with


DOI: 10.1021/ic503109a
*Inorg. Chem.* 2015, 54, 5634−5645

a certain degree of nondynamical correlation, which is described in different ways by different DFT methods.

The existence of the BS solution for CoP(NO) was also mentioned in ref 9, but it was concluded that the experimental structure and frequencies are better matched by nonhybrid functionals, leading to the SR solution only. This is also in agreement with the present findings (cf. Table 1). Pure functionals, in particular BP86, provide the best match with the experimental Co−N(O) distance and $\nu_{N-O}$ frequency, whereas hybrid functionals (leading to BS description) tend to overestimate the two parameters. The latter problem is most evident for B3LYP (20% of exact exchange), whereas for B3LYP* and TPSSh functionals (15% and 10%, respectively), the computed Co−N(O) distance is again very close to the experimental value (for TPSSh, in fact, even closer than for BP86), although $\nu_{N-O}$ is still overestimated by ∼100 $cm^{-1}$.[65] The failure of BS B3LYP calculations to reproduce the geometry and vibrational frequencies may be attributed to large spin contamination ($\langle S^2\rangle_{BS}$ = 0.61, compared with 0.30−0.35 obtained from B3LYP* and TPSSh), suggesting that B3LYP overestimates biradical character in the ground state of CoP(NO). The below discussion of NO binding energies will also confirm that B3LYP* and TPSSh are better suited to describe the Co−NO bond energy than standard B3LYP.

**NO Binding Energies.** *DFT versus Experimental Binding Energies.* Figure 3 reports the calculated NO binding energies

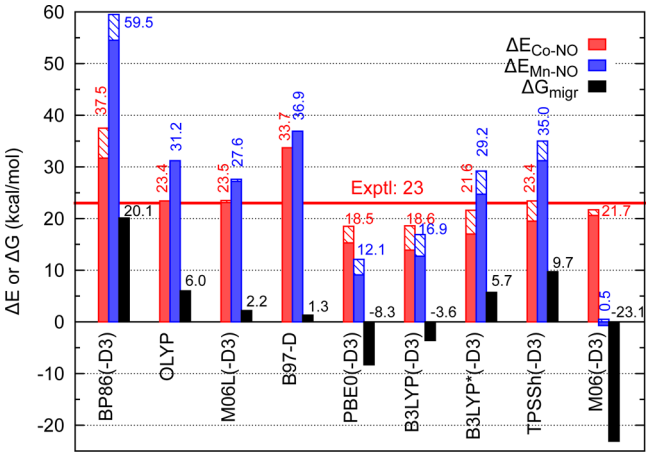


**Figure 3.** NO binding energies to CoP and MnP, and Gibbs energy of NO migration from MnP(NO) to CoP for a number of DFT methods, including dispersion correction (-D3) wherever possible; in such cases, the effect of dispersion is visually shown as the striped part of an M−NO bond energy bar, whereas only the dispersion-corrected value is numerically annotated. The experimental estimate of the Co−NO bond energy is shown as the solid horizontal line, whereas the nitrosyl migration experiment (reaction 1) indicates that $\Delta G_{migr} < 0$. The complete set of numeric results behind this plot can be found in Table S2, Supporting Information. Note that all hybrid DFT calculations for CoP(NO) as well as B3LYP(-D3) and PBE0(-D3) ones for MnP(NO) are BS, whereas other methods give only the SR solution.

to both metalloporphyrins ($\Delta E_{Co-NO}$ and $\Delta E_{Mn-NO}$) and Gibbs energy of NO migration ($\Delta G_{migr}$) according to eq 1. Before comparing theory with experiment, some comments must be made on both kinds of data. The computed $\Delta E_{M-NO}$ values are bond dissociation energies at $T$ = 0 K, computed with respect to ground spin states of the reactants: doublet for NO and CoP,[66] sextet for MnP,[67] and singlet for both nitrosyl complexes.[22,24b,68] These $\Delta E_{M-NO}$ values include ZPE corrections but do not include thermal and pressure effects contained in the experimental bond enthalpy, $\Delta H_{Co-NO}$ = 23.4 kcal/mol (ref19). However, the difference between $\Delta E_{Co-NO}$ (at $T$ = 0 K) and $\Delta H_{Co-NO}$ (at $T$ = 298 K, $p$ = 1 atm) computed for CoP(NO) using standard statistical thermodynamic approach is only 0.4 kcal/mol (see Table S5, Supporting Information). It means that the $\Delta E_{Co-NO}$ of 23 kcal/mol can be safely assumed as the experimental Co−NO binding energy, with a possible uncertainty of 1−2 kcal/mol, accounting also for the difference between the full TPP ring and its P model, and for the solvation effects omitted in the calculations. (As discussed in Computational Details, both effects are relatively small, on the order of 1 kcal/mol or smaller, and unimportant for the conclusions and interpretations presented in this work.) Concerning the Mn−NO bond energy, the precise experimental value is not available, but the nitrosyl migration experiment[21] indicates that $\Delta G_{migr}$ <0 (see Introduction). Note that since thermal and entropic effects are included in $\Delta G_{migr}$, it is clearly not equal to the straight difference of the two bond energies.

A number of DFT methods have been comparatively applied to provide the results in Figure 3. Among them, there are hybrid functionals with different percentages of the exact exchange (10% in TPSSh, 15% in B3LYP*, 20% in B3LYP, 25% in PBE0, and 27% in M06) because the amount of exact exchange is known to be the primary parameter affecting the performance of DFT methods for transition metal systems.[39,63,69] A typical trend[63] can be observed that pure functionals, i.e., not containing the exact exchange admixture, usually give larger binding energies than hybrid functionals, whereas for the latter functionals the binding energy tends to decrease with increasing admixture of the exact exchange. However, there are some exceptions. For instance, pure functionals OLYP and M06L give results comparable to those of hybrid functionals B3LYP* and TPSSh. Also M06 (containing as much as 27% admixture of the exact exchange) gives the Co−NO bond energy comparable to that of B3LYP* and TPSSh (containing only 15% and 10%). The above trends in DFT calculations, as well as considerable dependence of the results on the choice of functional, are qualitatively similar as were observed in related studies for Fe−porphyrin complexes.[11,12,18]

Wherever possible, the present results include the Grimme's dispersion correction (-D3).[31b] Significance of dispersion (van der Waals) interactions for the ligand binding energies to heme has been recently highlighted by Siegbahn et al.[17] Indeed, for most functionals employed here, the dispersion correction contributes as much as 3−5 kcal/mol to the metal−NO bond energies (the contribution of dispersion is shown in Figure 3 as a striped part of the respective bar). However, since the effect is very comparable for the two metals, the $\Delta G_{migr}$ values are nearly unaffected. The D3 correction is much smaller, at most ∼1 kcal/mol, for the Minnesota functionals (M06, M06L), whose parametrization includes noncovalent interactions to some extent.[36] Note also that B97-D already includes the dispersion correction in its definition, whereas no dispersion correction is available for OLYP, not allowing us to estimate the effect of dispersion correction for these two functionals.

The present calculations contain a number of improvements with respect to the previous study in ref 23. Here, not only are more DFT methods are tested (wherever possible including dispersion), but also ZPE corrections are appropriately included in the calculated bond energies, thermodynamic


DOI: 10.1021/ic503109a
Inorg. Chem. 2015, 54, 5634−5645

corrections are included in the $\Delta G_{migr}$ values, and relativistic effects are accounted for. Although these corrections are comparable for both metals, they do not cancel out completely in $\Delta G_{migr}$ (see Supporting Information). We further note that the present Co−NO bond energies calculated with B3LYP and TPSSh functionals are much larger than those reported previously[23] (i.e., 15.5 vs 3.9 and 21.0 vs 16.8 kcal/mol, respectively; ZPE-uncorrected values). This is because the present hybrid DFT results for CoP(NO) are from spin-projected BS calculations (see Computational Details). As can be found from the detailed comparison in Supporting Information (Tables S6−S7), switching from the SR to the BS solution has a significant stabilizing effect on the nitrosyl complex, particularly when spin contamination is corrected for (B3LYP, 11 kcal/mol; TPSSh, 5 kcal/mol), leading to the increase of the NO binding energy. Note that the large stabilizing effect of the spin-projection was also reported previously for isoelectronic Fe−$O_2$ complexes with heme groups.[11,17]

Notwithstanding all of the above improvements, a majority of the tested DFT and DFT-D3 methods still fail to predict the correct order of the two bond energies; hence, most of them point (incorrectly) to $\Delta G_{migr} > 0$. It is striking that the erroneously positive $\Delta G_{migr}$ is observed for all DFT methods which give the Co−NO bond energy nearly correct, i.e., for OLYP, M06L, M06L-D3, B3LYP*-D3, and TPSSh-D3. Only M06 and M06-D3 methods point to the correct Co−NO bond energy and simultaneously give $\Delta G_{migr} < 0$. However, these two methods yield the Mn−NO bond energy close to zero (without dispersion even negative), which does not agree with the stability of the pertinent complex under standard conditions. Also PBE0 and B3LYP functionals give $\Delta G_{migr} < 0$, but they significantly underestimate the Co−NO bond energy (even with dispersion included).[70] Finally, the B97-D functional gives $\Delta G_{migr} \approx 0$ (still positive though), but it overestimates the Co−NO bond energy by ∼10 kcal/mol.

Given all of the above, it looks like it is impossible to find a single DFT/DFT-D method which gives the correct Co−NO and Mn−NO bond energies simultaneously! This is surprising (although not entirely unusual in DFT calculations of metal−ligand bond energies; see, e.g., ref18) because a considerable error cancellation is expected when comparing energies of two similar bonds. Having recognized this problem, the solvation and possible limitations of the present porphin model (as compared with full tetraphenylporphyrin) were considered, but none of the mentioned effects turned out to be large and systematic enough to convincingly explain the above discrepancies of DFT calculations with the experimental data (see Computational Details).

*Role of Spin States.* The clue to understanding the above discrepancy is the difference in spin multiplicities of the ground state for both metalloporphyrins: doublet (low-spin) for Co(II) versus sextet (high-spin) for Mn(II).[66,67] The difference of spin state has profound consequences on the mechanism of NO binding, as can be illustrated by the calculated energy curves in Figure 4. For CoP(NO), the singlet ground state of the nitrosyl complex can be smoothly connected with the ground state of the dissociation products ($^2$CoP + $^2$NO), as shown in Figure 4a. Hence, NO binding to Co(II) porphyrin is a standard radical recombination, occurring on the ground state energy surface. Things are completely different for MnP(NO), where spin-crossing is required to connect the (low-spin) ground state of the nitrosyl complex with the (high-spin) ground state of the

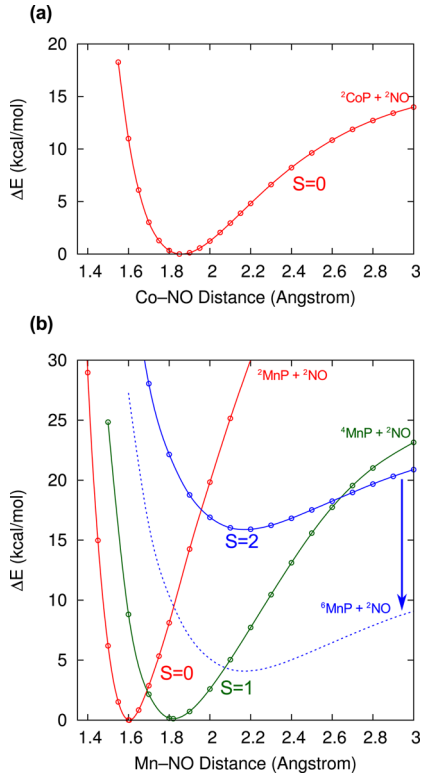


**Figure 4.** Energy curves for the dissociation of the metal−NO bond in (a) CoP(NO) and (b) MnP(NO) complexes at the unrestricted B3LYP*/def2-SV(P) level with indicated spin states of the fragments in different dissociation limits. The dashed line for MnP(NO) is the (S = 2) curve shifted down by 12 kcal/mol with respect to the (S = 0) curve to correct the error of the B3LYP* functional on the relative energy of the dissociation limits of both curves, based on the relative energy of $^{2,6}$MnP spin states; this is a graphical representation of the SSE correction (see text), in this case decreasing the bond energy.

dissociation products ($^6$MnP + $^2$NO); see Figure 4b. In fact, to bind NO to the high-spin ground state of MnP, the spin state needs to change twice: first by crossing from the quintet to the triplet and second to the singlet state.[71]

It is well known from the literature[72,73] that crossing of energy surfaces along a reaction path may strongly affect the kinetics. Herein, the experimental data suggest that NO recombination with Mn(TPP) is ∼100 times slower than that with Co(TPP).[21,74] Already in 1989, Hoshino and Kogure hypothesized that this slowness may be caused by the change of Mn spin state.[74] Later on, Kubiak et al. reported the complex (biexponential) kinetic behavior of NO recombination with Mn(TPP).[21] Recently, Kurtikyan et al. suggested that the complex kinetic behavior observed by Kubiak et al. may be due to the existence of a relatively stable triplet isomer of Mn(TPP)(NO), which they discovered in amorphous solid phase.[55] The equilibrium geometry of this triplet state has a bent MnNO motif and corresponds to the deep minimum on the (S = 1) curve in Figure 4b. (Note that the triplet isomer is slightly overstabilized by the B3LYP* functional which was used for energy curves in Figure 4; according to the experimental data, Mn(TPP)(NO) is the singlet ground state,[22] the triplet lying ∼1 kcal/mol above.[55])

Although the triplet isomer is already associated and its formation should be fast, i.e., there is no barrier on crossing from the (S = 2) to (S = 1) curve in Figure 4b, the experimental kinetic data of NO recombination more probably


DOI: 10.1021/ic503109a
*Inorg. Chem.* 2015, 54, 5634−5645

Table 2. Adiabatic Relative Energies of Spin States $^2$MnP and $^4$MnP with Respect to $^6$MnP Ground State[a]

| | CCSD(T) | PBE0 | B3LYP | B3LYP* | TPSSh | M06 | M06L | OLYP |
|---|---|---|---|---|---|---|---|---|
| $^4$MnP | 10.3 | 7.2 | 2.4 | −1.0 | −1.6 | 14.7 | 11.2 | 4.2 |
| $^2$MnP | 45.7 | 49.7 | 38.5 | 33.9 | 33.9 | 63.8 | 53.8 | 45.1 |
| error on energy of reaction 5[b] | | −4.0 | 7.2 | 11.8 | 11.8 | −18.1 | −8.1 | 0.6 |

[a]Electronic energies, kcal/mol. The electronic states for $^{2,4,6}$MnP are $^2E_g$, $^4A_{2g}$, and $^6A_{1g}$, respectively. [b]With respect to the CCSD(T) data, treated as reference; this number (times −1) gives the SSE correction to the Mn−NO bond energy (see text).

reflect the rate of formation of the singlet ground state.[75] As seen in Figure 4b, when going from the triplet (intermediate) to singlet isomer (final product), there is an energy barrier to surpass. This barrier may be more accurately calculated to be 2.6 kcal/mol based on the minimum energy crossing point (MECP) optimization using the TPSSh-D3 method because this method gives the relative energy of the crossing spin states in agreement with the experimental thermal equilibrium behavior.[55] (The optimized structures and relative energies of both spin states and their MECP can be found in Figure S2, Supporting Information.) The present barrier seems to be roughly consistent with ∼100 times slower recombination for Mn than for Co complexes. It is also comparable to the barrier reported by Harvey for carbon monoxide recombination in the myoglobin model (2.5 kcal/mol),[13a] where there is also a change of spin state during the ligand binding to Fe(II), although no stable intermediate is formed.

Nonetheless, more important to highlight in this contribution is that the change of spin state for the Mn complex has also *thermochemical consequences*. This is because the Mn−NO bond energy, unlike the Co−NO one, contains the cost of spin promotion from the high-spin to the low-spin state. In other words, when calculating the Mn−NO bond energy, one takes the energy of the complex from the low-spin energy surface, whereas the energy of the dissociation limit is from the high-spin surface. This makes the Mn−NO bond energy influenced by known inaccuracies of common DFT methods in reproducing the metal spin-state energetics.[76]

To appreciate the latter fact, it is advantageous to consider the Mn−NO bond dissociation

$$^1[\mathrm{MnP(NO)}] \rightarrow {}^6\mathrm{MnP} + {}^2\mathrm{NO} \quad (3)$$

in two virtual steps:

$$^1[\mathrm{MnP(NO)}] \rightarrow {}^2\mathrm{MnP} + {}^2\mathrm{NO} \quad (4)$$

$$^2\mathrm{MnP} \rightarrow {}^6\mathrm{MnP} \quad (5)$$

The first step (eq 4) is "adiabatic" dissociation occurring on a single (low-spin) energy surface; the second step (eq 5) is spin-state conversion of MnP, i.e., switching from the excited (low-spin) to the ground state (high-spin) energy surface in the dissociation limit. According to Hess's law, the energies of reactions 4 and 5 sum up to the energy of reaction 3, but it may be difficult to get both contributions simultaneously correct from a single DFT calculation. Indeed, the previous experience indicates that a much larger admixture of exact exchange may be necessary to correctly describe the spin-state conversion energy of a metalloporphyrin complex[30,77] than to describe an energy of a highly covalent M−NO bond.[12,18,78] This sensitivity of DFT results to the exact exchange admixture is empirically well known[39,79,80] and attributed to a tricky description of nondynamical correlation in approximate DFT methods[63,69] (see also above). Because reaction 4 is analogous, in terms of the reactants' spin states and covalent character of the M−NO bond, to the dissociation of CoP(NO), it is reasonable to look for suitable DFT methods to describe the energy of reaction 4 among those which are successful in describing the Co−NO bond energy. However, not all of these DFT methods are appropriate for describing the spin-state conversion reaction 5.

How severe this problem is can be assessed by looking at relative energies of the MnP spin states computed at the DFT level in comparison with accurate wave function calculations at the CCSD(T) level (Table 2). It follows that the DFT description of reaction 5 energy is far from being perfect, in particular for some functionals which (after correcting for dispersion) give good results for the Co−NO bond energy. For instance, the B3LYP* and TPSSh functionals overstabilize the low-spin state ($^2$MnP) with respect to the high-spin state ($^6$MnP) by more than 10 kcal/mol, while M06 errs in the opposite direction by nearly 20 kcal/mol. Thus, even if these functionals (corrected for dispersion) may be able to reproduce the energy of reaction 4, there still remains a problem with reaction 5. In other words, the Mn−NO bond energy may be either overestimated or underestimated due to the error on the spin-state energetics of MnP. Having recognized this problem, one may consider a scheme in which the energy of reaction 4 is taken from DFT/DFT-D calculations, whereas the energy of reaction 5 is taken from a higher level method, such as CCSD(T). This is, clearly, equivalent to correcting the dissociation energy (reaction 3) obtained from standard DFT/DFT-D calculation for an error of a given functional on the relative spin-state energetics of $^{2,6}$MnP, taken from Table 2. This simple scheme will be called here the *spin-state energy (SSE) correction* to DFT/DFT-D calculations.

The above assumption that the energy of low-spin dissociation (reaction 4) can be correctly reproduced by some DFT(-D3) methods (even if the real dissociation energy is incorrect due to the problem with the spin-state conversion energy) can be put equivalently in different words: both low-spin species, $^1$MnP(NO) and $^2$MnP, are comparably over-stabilized/understabilized (depending on functional) with respect to the corresponding high-spin species, $^6$MnP+$^2$NO and $^6$MnP; hence, a big part of the DFT error in the energy of reaction 3 can be approximated by the error in the energy of reaction 5. Whether this assumption is satisfied (and for which functionals), will be verified a posteriori by comparison with the CCSD(T) estimate of the Mn−NO bond energy (see below).

Applying the SSE correction may be also represented graphically in Figure 4b as vertical shifting of the low-spin and high-spin curves with respect to each other, in order to correct an energy separation between their dissociation limits (one containing $^2$MnP and the other $^6$MnP). In the example shown in Figure 4b, the energy curves were computed using the B3LYP* functional, which overstabilizes the $^2$MnP spin state with respect to $^6$MnP by ∼12 kcal/mol (cf. Table 2). Therefore, the high-spin curve needs to be shifted with respect to the low-spin curve down in energy by ∼12 kcal/mol to correct the relative spin state energetics of $^{2,6}$MnP in the



DOI: 10.1021/ic503109a
Inorg. Chem. 2015, 54, 5634−5645

dissociation limits. This is, clearly, equivalent to reducing the normally calculated Mn−NO bond energy by the same amount of energy (i.e., the SSE correction for B3LYP*).

Table 3 contains the DFT results after including the proposed SSE correction to the Mn−NO bond energy. The table is restricted to those DFT methods which give the Co−NO bond energy close to the experimental value. Note that without the SSE correction none of them gives the correct Mn−NO bond energy because either strong underbinding (M06) or overbinding (other methods) is observed (cf. Figure 3). However, after including the SSE correction a considerable improvement is observed for hybrid methods: B3LYP*-D3, TPSSh-D3, and M06-D3. Now all of them point to $\Delta G_{migr} < 0$, in qualitative agreement with the NO migration experiment. The success of these SSE-corrected results in reproducing the correct sign of $\Delta G_{migr}$ and their reasonably good agreement with the high-level CCSD(T) estimate (also included in Table 3; see below for more details) confirm that the B3LYP*-D3, TPSSh-D3, and M06-D3 methods give the correct energy of low-spin dissociation of MnP(NO) (reaction 4), which was the basic assumption behind the SSE correction. It is thus believed that these three hybrid functionals, once supplemented with the Grimme's dispersion correction and with the SSE correction, provide the best description of NO binding energy to the considered metalloporphyrins. (Note that structural and vibrational parameters of both nitrosyl complexes are also nicely reproduced by B3LYP* and TPSSh functionals, and not so well by M06.) The analogous improvement in NO binding energies is not observed for pure DFT methods, OLYP and M06L-D3; in the latter case, the SSE correction actually deteriorates the results. It is also noteworthy that for OLYP the SSE correction is close to zero, but this method still overbinds the Mn−NO complex as compared with the Co−NO one. Therefore, it must be concluded that OLYP and M06L-D3 overestimate the Mn−NO bond energy for different reasons other than being due to an error on the Mn(II) spin-state energetics. The SSE correction is not helpful for these pure functionals because they overestimate the low-spin dissociation energy of MnP(NO) (the energy of reaction 4 and the well depth of the S = 0 state in Figure 4b), despite being accurate for analogous low-spin dissociation of CoP(NO). This failure may be due to an unsatisfactory description of nondynamical correlation in the Mn−NO bond, compared with that in the Co−NO bond.

**Table 3. Binding Energies of NO to CoP and MnP, and Gibbs Energy of NO Migration after Including Spin-State Energy (SSE) Correction for Mn[a]**

| | $\Delta E_{Co-NO}$ | $\Delta E_{Mn-NO}$ | $\Delta G_{migr}$ |
|---|---|---|---|
| B3LYP*-D3 + SSE | 21.6 | 17.4 | −6.1 |
| TPSSh-D3 + SSE | 23.4 | 23.2 | −2.1 |
| M06-D3 + SSE | 21.7 | 18.9 | −4.2 |
| OLYP + SSE | 23.4 | 30.6 | 5.3 |
| M06L-D3 + SSE | 23.5 | 35.7 | 10.3 |
| CCSD(T) estimates[b] | 25.1 | 20.7 | −6.3 |
| CASPT2 | 23.1[c] | | |
| experiment | 23 | | <0 |

[a]In kcal/mol. The SSE corrections are from Table 2. Note that B3LYP*, TPSSh, and M06 functionals point to the BS solution for CoP(NO); the respective results are corrected for spin contamination. [b]Estimates based on the small mimics (see Computational Details and Supporting Information). [c]From ref 81.

Although OLYP calculations reproduce the Co−NO bond energy quite well, it must be noticed that they do not contain the dispersion correction (because it is not available for OLYP). One can assume that the missing effect of dispersion will be on the order of 3−5 kcal/mol (i.e., similar to those found for BP86, PBE0, B3LYP, or TPSSh functionals, which, likewise OLYP, have not been explicitly parametrized to account the dispersion). Taking this into account, the success of OLYP for the Co−NO bond energy is not unequivocal. It should be rather viewed as the compensation of two errors: an unsatisfactory treatment of dispersive interactions and a known tendency of pure functionals to overbind.[63] This error compensation works, apparently, much worse for the Mn−NO than for the Co−NO bond energy, explaining why OLYP cannot reproduce the former energy, although it gives a good result for the latter one. Goodrich et al. also criticized the performance of OLYP in their study of *trans* effect in heme compounds,[18] although previous experience favored OLYP for the description of ligand binding to heme.[11]

*Comparison with Accurate Coupled-Cluster Calculations.* For additional confirmation, estimates of the NO binding energies were obtained from reliable coupled-cluster calculations at the CCSD(T) level. As explained in Computational Details, the CCSD(T) calculations were carried out for simplified mimics $ML_2(NO)$ based on which the results for MP(NO) were estimated with aid of the extrapolation procedure.[30] Only these final estimates are included in Table 3, whereas the interested reader is pointed to Supporting Information for the details (Table S12 and Figure S5).

Looking at Table 3, one notices immediately that the CCSD(T) estimate of the Co−NO bond energy in CoP(NO) is within 2 kcal/mol in agreement with the experimental data. This should be considered a very satisfactory agreement, given the approximate character of the extrapolation procedure used to obtain this number. The analogous estimate of the Mn−NO bond energy is smaller by 4 kcal/mol, which leads to the negative estimate of $\Delta G_{migr}$, in accord with the experiment.[21] The CCSD(T) estimates also agree up to a few kcal/mol with the SSE-corrected B3LYP*-D3, TPSSh-D3, and M06-D3 results (see above). Either these SSE-corrected DFT results or the CCSD(T) estimates confirm that the Mn−NO bond is weaker (i.e., has smaller a dissociation energy) than the Co−NO bond.

Concerning the accuracy of the present CCSD(T) calculations, it is noteworthy that the total basis set superposition error (BSSE) on the M−NO bond energies amounts to only ∼2 kcal/mol for both mimics (cf. Table S12, Supporting Information). This is to be compared with previous ab initio calculations of ligand binding energies (at CASPT2 level), where the BSSE corrections were as large as 7−9 kcal/mol (ref 11) or even ∼22 kcal/mol (ref 81). The current, much smaller BSSE values represent a remarkable improvement, suggesting that basis set error is not an issue in the present calculations. Furthermore, some diagnostics of multireference character (intended to examine whether a single-reference treatment is appropriate[82]) are summarized in Table S13, Supporting Information. The most widely used $T_1$ and $D_1$ diagnostics are based on amplitudes of single excitations and thus provide a measure of orbital relaxation in response to the electronic correlation. All $T_1$ diagnostics are below the recently suggested threshold of 0.05,[82] except for $CoL_2(NO)$ (0.06).



DOI: 10.1021/ic503109a
Inorg. Chem. 2015, 54, 5634−5645

The $D_1$ diagnostics is equal to the suggested threshold of 0.15[82] in the case of $CoL_2$ and exceeds it in the case of $MnL_2(NO)$ (0.17) and $CoL_2(NO)$ (0.43). The large value in the latter case is due to the relaxation of orbitals describing the Co−NO $\sigma$ bond (Table S14−S15 and Figure S6, Supporting Information), which is not unexpected in view of the biradical character evidenced by the above BS DFT calculations. In spite of that, the resulting estimate of the Co−NO bond energy is close to the experimental value and to the previous multireference (CASPT2) calculations.[81] This suggests that the moderate multireference character of these nitrosyl complexes is correctly accounted for in the present CCSD(T) treatment. There are also many cases in the literature where CCSD(T) provides reliable results despite significant $T_1/D_1$ diagnostics.[26] However, it would be worthy to revisit these challenging systems in the future by performing even more advanced ab initio calculations (also because the present CCSD(T) data for MP(NO) complexes are mere estimates).

**Structure−Energy Relationship.** Last but not least, nitrosyl complexes of Co(II) and Mn(II) porphyrins are interesting because they contradict the paradigm of correlation between structure and thermochemistry. This paradigm says that when comparing two similar bonds, the shorter bond (the one with a shorter bond distance) will be also the stronger bond (the one with a larger dissociation energy). This paradigm may be extremely successful in many areas, such as for the analysis of intermolecular interactions based on purely structural data, when the term "interaction" (referring to bond energy) and "short contact" (referring to bond distance) are quite often used interchangeably. The same paradigm also works very well in typical organic chemistry problems, explaining the structure−energy relationship between single, double, and triple bonds linking the same kind of atoms. Here, however, when discussing metal−NO bonding, we need to clearly distinguish the concept of bond distance ("tightness") from the concept of bond energy ("strength").

Indeed, in the sense of M−N(O) distance, the NO ligand is more tightly bound to the Mn (∼1.6 Å) than to the Co (∼1.8 Å) center in the respective porphyrin complexes, and the same holds true about the $\nu_{M-NO}$ stretching frequencies (cf. Table 1). However, the Mn−NO bond is weaker (in the energetic sense) than the Co−NO one. The latter fact is clearly revealed from the experimental data ($\Delta G_{migr} < 0$)[21] and confirmed by high-level calculations reported herein (cf. Table 3). One should note a similarity between the present case and the case of Fe(III)−porphyrin NO complexes described by Praneeth et al., where the nitrosyl is tightly bound (from the structure and IR spectroscopy), although the bond is weak (from thermodynamics).[25] The explanation of the present tightness/strength dichotomy is also similar to that given by Praneeth et al.: the effect is due to the crossing of spin-states along the Mn−NO dissociation path (cf. Figure 4b).

First of all, the lower bond energy in the case of the Mn complex should not be entirely surprising since binding energy is dependent not only on the properties of the complex but also on the dissociation products. The equilibrium parameters of MnP(NO) reflect the great well depth of the low-spin energy curve, corresponding to the $^2$MnP + $^2$NO dissociation limit. Provided that the complex could be dissociated "adiabatically," i.e., to $^2$MnP + $^2$NO along this low-spin energy surface, the Mn−NO bond would be much stronger than the Co−NO one, in full accord with a shorter M−N(O) bond distance and a higher $\nu_{M-NO}$ vibrational frequency (cf. Figure 4b). However, the real dissociation limit is $^6$MnP + $^2$NO, which is much below the $^2$MnP + $^2$NO one. This makes the actual Mn−NO bond energy, computed with respect to the correct dissociation limit ($^6$MnP + $^2$NO), much lower than that expected based on the MnP(NO) equilibrium parameters.

Note, however, that there is an additional caveat for the present case: most of the standard DFT calculations point to $\Delta E_{Mn-NO} > \Delta E_{Co-NO}$. This is an incorrect result, although (at first sight) it seems to correlate with the shorter Mn−NO distance.[23] However, as was shown above, most of the DFT methods, while capable of describing the structures correctly, have large errors on the calculated binding energies, and only after including the necessary correction for the Mn(II) spin-state energetics, a few DFT methods turned out to be capable of providing the correct Co−NO and Mn−NO bond energies simultaneously. Not appreciating this effect may thus easily lead to a *wrong* conclusion from the routine DFT approach: that the Mn−NO bond is thermodynamically stronger in accord with the fact that it is shorter.

## CONCLUSIONS

The structural and energetic aspects of NO binding to Co(II) and Mn(II) sites in porphyrins was studied by high-level theoretical calculations (DFT, DFT-D, and coupled-cluster CCSD(T)) and critically discussed in relation to the available experimental results (structures, vibrational frequencies, and thermochemical and kinetic data). The crossing of spin states concerted with the formation of the Mn−NO bond was highlighted and shown here to have not only kinetic but also thermochemical consequences. The latter ones arise from the fact that the spin-state conversion energy contributes to the Mn−NO bond energy (but not to the Co−NO bond energy). Recognizing this role of spin states in the ligand binding properties turned out to be crucial to the correct interpretation of the experimental and computational results for the studied metalloporphyrin complexes.

The experience gathered in this work indicated that describing the spin-state conversion energy on equal footing with the covalent bonding effect remains a considerable challenge for DFT and DFT-D methods. Most of them, including functionals widely used in the field of bioinorganic chemistry, incorrectly predict that the Mn−NO bond has a larger dissociation energy than the Co−NO bond, and thus, they fail to reproduce the relative thermodynamic stabilities of the studied nitrosyl complexes, as determined by IR spectroscopy. Only after including the proposed (spin-state energy) correction to the Mn−NO bond energy, just a few DFT methods (B3LYP*-D3, TPPSh-D3, and M06-D3) out of many explored in this work, were able to yield the Mn−NO and Co−NO bond energies in agreement with the experimental data and the reliable estimates from wave function theory (CCSD(T)). The risk of incorrect interpretation of the experimental data by relying on inaccurate computational results was pointed out. It is worth noting in passing that, given the lack of a precise experimental value of the Mn−NO bond energy and a big methodological challenge in computing it accurately, it would be very interesting to compare the presently calculated data with reliable gas-phase binding energies (like those obtained recently[6] by ion cyclotron resonance for Fe−porphyrin complexes with CO and $O_2$; such gas-phase data are currently unavailable for the analogous Mn(II) and Co(II) complexes with NO).



DOI: 10.1021/ic503109a
*Inorg. Chem.* 2015, 54, 5634−5645

This work also confirmed that the Mn−NO and Co−NO bond energies, if determined correctly, i.e., in accord with the experimental data, *do not* correlate with the structures of the studied complexes in the expected way: the shorter (1.6 Å) Mn−NO bond is thermodynamically less stable than the longer (1.8 Å) Co−NO bond! It was shown that this paradox can be explained by recalling the change of Mn spin state accompanying the coordination of the NO, and the resulting energy contribution (due to spin-state conversion energy) to the Mn−NO bond dissociation energy. Thus, in regard to the title question, whether a tighter binding always stronger, the answer is clearly negative. When multiple spin states are involved in a ligand binding process (which is not unusual in bioinorganic chemistry), the paradigmatic relationship between structural chemistry (bond length) and thermochemistry (bond energy) may not be obeyed because a part of the bond energy is due to the spin-state conversion energy, and the latter portion of energy is hardly reflected in the structural parameters.

## ■ ASSOCIATED CONTENT

### Supporting Information

Details of DFT and CCSD(T) calculations, including Cartesian atomic coordinates, and complete ref 32. The Supporting Information is available free of charge on the ACS Publications website at DOI: 10.1021/ic503109a.

## ■ AUTHOR INFORMATION


### Corresponding Author

*E-mail: mradon@chemia.uj.edu.pl.


### Notes

The authors declare no competing financial interest.

## ■ ACKNOWLEDGMENTS

I am thankful to Professor Clifford Kubiak (UCSD) for valuable comments concerning the experimental results in ref 21, and to Professor Ewa Broclawik and Professor Tomasz Borowski (IKiFP PAN) for helpful discussions on this work. This research was supported by grant IP2011 044471 from Ministry of Science and Higher Education, Poland; by PLGrid infrastructure, POWIEW project, and Wroclaw Centre for Networking and Supercomputing (grant no. 181); and by the COST action CM1305 ECOSTBio.

## ■ REFERENCES


(1) Springer, B. A.; Sligar, S. G.; Olson, J. S.; Phillips, G. N. J. *Chem. Rev.* **1994**, *94*, 699−714.

(2) Traylor, T. G.; Sharma, V. S. *Biochemistry* **1992**, *31*, 2847−2849.

(3) (a) Shaik, S.; Cohen, S.; Wang, Y.; Chen, H.; Kumar, D.; Thiel, W. *Chem. Rev.* **2010**, *110*, 949−1017. (b) Denisov, I. G.; Makris, T. M.; Sligar, S. G.; Schlichting, I. *Chem. Rev.* **2005**, *105*, 2253−2278.

(4) Perutz, M. F.; Fermi, G.; Luisi, B.; Shaanan, B.; Liddington, R. C. *Acc. Chem. Res.* **1987**, *20*, 309−321.

(5) (a) Blomberg, L. M.; Blomberg, M. R.; Siegbahn, P. E. *J. Inorg. Biochem.* **2005**, *99*, 949−958. (b) Kepp, K. P.; Dasmeh, P. *J. Phys. Chem. B* **2013**, *117*, 3755−3770.

(6) Karpuschkin, T.; Kappes, M. M.; Hampe, O. *Angew. Chem., Int. Ed.* **2013**, *52*, 10374−10377.

(7) (a) Angelelli, F.; Chiavarino, B.; Crestoni, M. E.; Fornarini, S. *J. Am. Soc. Mass Spectrom.* **2005**, *16*, 589−598. (b) Chiavarino, B.; Crestoni, M. E.; Fornarini, S.; Rovira, C. *Inorg. Chem.* **2008**, *47*, 7792−7801. (c) Lanucara, F.; Scuderi, D.; Chiavarino, B.; Fornarini, S.; Maitre, P.; Crestoni, M. E. *J. Phys. Chem. Lett.* **2013**, *4*, 2414−2417.

(8) Chen, O.; Groh, S.; Liechty, A.; Ridge, D. P. *J. Am. Chem. Soc.* **1999**, *121*, 11910−11911.

(9) Soldatova, A. V.; Ibrahim, M.; Spiro, T. G. *Inorg. Chem.* **2013**, *52*, 7478−7486.

(10) Rovira, C.; Kunc, K.; Hutter, J.; Ballone, P.; Parrinello, M. *J. Phys. Chem. A* **1997**, *101*, 8914−8925.

(11) Radoń, M.; Pierloot, K. *J. Phys. Chem. A* **2008**, *112*, 11824−11832.

(12) Olah, J.; Harvey, J. *J. Phys. Chem. A* **2009**, *113*, 7338−7345.

(13) (a) Harvey, J. N. *J. Am. Chem. Soc.* **2000**, *122*, 12401−12402. (b) Strickland, N.; Harvey, J. N. J. *Phys. Chem. B* **2007**, *111*, 841−852.

(14) (a) Chen, H.; Ikeda-Saito, M.; Shaik, S. *J. Am. Chem. Soc.* **2008**, *130*, 14778−14790. (b) Shaik, S.; Chen, H. *J. Biol. Inorg. Chem.* **2011**, *16*, 841−855.

(15) Radoń, M.; Broclawik, E.; Pierloot, K. *J. Phys. Chem. B* **2010**, *114*, 1518−1528.

(16) Lehnert, N.; Scheidt, W.; Wolf, M. In *Nitrosyl Complexes in Inorganic Chemistry, Biochemistry and Medicine II*; Mingos, D. M. P, Ed.; Structure and Bonding; Springer: Berlin, Germany, 2014; Vol. *154*; pp 155−223.

(17) Siegbahn, P. E. M.; Blomberg, M. R. A.; Chen, S.-L. *J. Chem. Theory Comput.* **2010**, *6*, 2040−2044.

(18) Goodrich, L. E.; Lehnert, N. *J. Inorg. Biochem.* **2013**, *118*, 179−186.

(19) Zhu, X.-Q.; Li, Q.; Hao, W.-F.; Cheng, J.-P. *J. Am. Chem. Soc.* **2002**, *124*, 9887−9893.

(20) Wayland, B. B.; Olson, L. W.; Siddiqui, Z. U. *J. Am. Chem. Soc.* **1976**, *98*, 94−98.

(21) Zavarine, I. S.; Kini, A. D.; Morimoto, B. H.; Kubiak, C. P. *J. Phys. Chem. B* **1998**, *102*, 7287−7292.

(22) Scheidt, W. R.; Hatano, K.; Rupprecht, G. A.; Piciulo, P. L. *Inorg. Chem.* **1979**, *18*, 292−299.

(23) Jaworska, M.; Lodowski, P. *Struct. Chem.* **2012**, *23*, 1333−1348.

(24) (a) Ellison, M. K.; Scheidt, W. R. *Inorg. Chem.* **1998**, *37*, 382−383. (b) Scheidt, W. R.; Hoard, J. L. *J. Am. Chem. Soc.* **1973**, *95*, 8281−8288. (c) Richter-Addo, G. B.; Hodge, S. J.; Yi, G.-B.; Khan, M. A.; Ma, T.; Van Caemelbecke, E.; Guo, N.; Kadish, K. M. *Inorg. Chem.* **1996**, *35*, 6530−6538. (d) Richter-Addo, G. B.; Hodge, S. J.; Yi, G.-B.; Khan, M. A.; Ma, T.; Van Caemelbecke, E.; Guo, N.; Kadish, K. M. *Inorg. Chem.* **1997**, *36*, 2696−2696.

(25) (a) Goodrich, L. E.; Paulat, F.; Praneeth, V. K. K.; Lehnert, N. *Inorg. Chem.* **2010**, *49*, 6293−6316. (b) Praneeth, V. K. K.; Paulat, F.; Berto, T. C.; George, S. D.; Näther, C.; Sulok, C. D.; Lehnert, N. *J. Am. Chem. Soc.* **2008**, *130*, 15288−15303.

(26) (a) Harvey, J. N. *J. Biol.Inorg. Chem.* **2011**, *16*, 831−839. (b) Neese, F.; Liakos, D.; Ye, S. *J. Biol. Inorg. Chem.* **2011**, *16*, 821−829.

(27) Petit, A. S.; Pennifold, R. C. R.; Harvey, J. N. *Inorg. Chem.* **2014**, *53*, 6473−6481.

(28) (a) Sigfridsson, E.; Ryde, U. *J. Biol. Inorg. Chem.* **2003**, *8*, 273−282. (b) Jensen, K. P.; Ryde, U. *ChemBioChem* **2003**, *4*, 413−424.

(29) Ghosh, A.; Persson, B. J.; Taylor, P. R. *J. Biol. Inorg. Chem.* **2003**, *8*, 507−511.

(30) Radoń, M. *J. Chem. Theory Comput.* **2014**, *10*, 2306−2321.

(31) (a) Grimme, S. *Willey Interdiscip. Rev. Comp. Mol. Sci.* **2011**, *1*, 211−228. (b) Grimme, S.; Antony, J.; Ehrlich, S.; Krieg, H. *J. Chem. Phys.* **2010**, *132*, 154104. (c) Grimme, S. *J. Comput. Chem.* **2006**, *27*, 1787−1799.

(32) Frisch, M. et al. *Gaussian 09*, revision C.01; Gaussian Inc.: Wallingford, CT, 2009.

(33) TURBOMOLE V6.4−6.5 (2012−2013), a Development of University of Karlsruhe and Forschungszentrum Karlsruhe GmbH, 1989−2007, TURBOMOLE GmbH, since 2007; available from http://www.turbomole.com (accessed Aug 2014).

(34) (a) Becke, A. D. *Phys. Rev. A* **1988**, *38*, 3098−3100. (b) Perdew, J. P. *Phys. Rev. B* **1986**, *33*, 8822−8824.

(35) Handy, N. C.; Cohen, A. J. *Mol. Phys.* **2001**, *99*, 403−412.

(36) (a) Zhao, Y.; Truhlar, D. G. *J. Chem. Phys.* **2006**, *125*, 194101. (b) Zhao, Y.; Truhlar, D. G. *Theor. Chem. Acc.* **2008**, *120*, 215−241.




DOI: 10.1021/ic503109a
*Inorg. Chem.* 2015, 54, 5634−5645

(37) Perdew, J. P.; Ernzerhof, M.; Burke, K. *J. Chem. Phys.* **1996**, *105*, 9982−9985.
(38) (a) Becke, A. D. *J. Chem. Phys.* **1993**, *98*, 5648−5652. (b) Stephens, P. J.; Devlin, F. J.; Chabalowski, C. F.; Frisch, M. J. *J. Phys. Chem.* **1994**, *98*, 11623−11627.
(39) (a) Reiher, M.; Salomon, O.; Hess, B. A. *Theor. Chem. Acc.* **2001**, *107*, 48−55. (b) Salomon, O.; Reiher, M.; Hess, B. A. *J. Chem. Phys.* **2002**, *117*, 4729−4737.
(40) Perdew, J. P.; Tao, J.; Staroverov, V. N.; Scuseria, G. E. *J. Chem. Phys.* **2004**, *120*, 6898−6911.
(41) Reiher, M.; Wolf, A. *J. Chem. Phys.* **2004**, *121*, 10945−10956.
(42) (a) Neese, F. *J. Phys. Chem. Solids* **2004**, *65*, 781−785. (b) Neese, F. *Coord. Chem. Revs* **2009**, *253*, 526−563.
(43) For MnP(NO) and the M06 functional, when the initial guess and geometry are taken from the PBE0 BS solution ($\langle S^2 \rangle$ = 0.41), a slight BS character is seen after converging SCF in the first geometry cycle ($\langle S^2 \rangle$ = 0.05), but it totally disappears in subsequent geometry cycles, whereas the energy is lowered. It is also remarkable that even for PBE0, where the BS character is most pronounced, the electronic Hessian for the SR solution has only positive eigenvalues; thus, the standard stability test fails to detect the presence of the lower-energy BS solution in the case of MnP(NO). Note that the stability test detects the presence of the BS solution successfully in the case of CoP(NO).
(44) (a) Yamaguchi, K.; Takahara, Y.; Fueno, T.; Houk, K. *Theor. Chim. Acta* **1988**, *73*, 337−364. (b) Takahara, Y.; Yamaguchi, K.; Fueno, T. *Chem. Phys. Lett.* **1989**, *157*, 211−216.
(45) (a) Malykhin, S. E.; Volodin, A. M.; Zhidomirov, G. M. *Appl. Magn. Reson.* **2008**, *33*, 153−166. (b) Rodriguez, J. H.; McCusker, J. K. *J. Chem. Phys.* **2002**, *116*, 6253−6270.
(46) (a) Bearpark, M. J.; Robb, M. A.; Schlegel, H. B. *Chem. Phys. Lett.* **1994**, *223*, 269−274. (b) Harvey, J. N.; Aschi, M.; Schwarz, H.; Koch, W. *Theor. Chem. Acc.* **1998**, *99*, 95−99.
(47) MECPy − Program and Library in Python for Performing Geometry Optimization to Minimum and Minimum Energy Crossing Point (MECP), in Cartesian and Internal Coordinates. Available from: www.chemia.uj.edu.pl/~mradon/mecpy (accessed Mar 2015).
(48) Klamt, A. *J. Phys. Chem.* **1995**, *99*, 2224−2235.
(49) Judging the stabilities of the adducts, one should note that, unlike the final set of M−NO bond energies (Figure 3 and Table 3), the solvent binding energies discussed here are not corrected for BSSE and ZPE effects and therefore are overestimated by probably a few kcal/mol. One should also mind the entropic contribution to Gibbs free energy of solvent binding, which makes the formation of an adduct less favorable than that according to pure energy analysis by ∼10 kcal/mol.
(50) (a) Werner, H.-J. et al. *MOLPRO: A Package of Ab Initio Programs*, version 2012.1; University College Cardiff Consultants Limited: Cardiff, South Glamorgan , Wales, U.K., 2012; see http://www.molpro.net. (b) Werner, H.-J.; Knowles, P. J.; Knizia, G.; Manby, F. R.; Schütz, M. *WIREs Comput. Mol. Sci.* **2012**, *2*, 242−253.
(51) (a) Knowles, P. J.; Hampel, C.; Werner, H.-J. *J. Chem. Phys.* **1993**, *99*, 5219−5227. (b) Knowles, P. J.; Hampel, C.; Werner, H.-J. *J. Chem. Phys.* **2000**, *112*, 3106−3107.
(52) (a) Adler, T. B.; Knizia, G.; Werner, H.-J. *J. Chem. Phys.* **2007**, *127*, 221106. (b) Knizia, G.; Adler, T. B.; Werner, H.-J. *J. Chem. Phys.* **2009**, *130*, 054104.
(53) (a) Hättig, C.; Klopper, W.; Köhn, A.; Tew, D. P. *Chem. Rev.* **2012**, *112*, 4−74. (b) Kong, L.; Bischoff, F. A.; Valeev, E. F. *Chem. Rev.* **2012**, *112*, 75−107.
(54) Cordero, B.; Gomez, V.; Platero-Prats, A. E.; Reves, M.; Echeverria, J.; Cremades, E.; Barragan, F.; Alvarez, S. *Dalton Trans.* **2008**, 2832−2838.
(55) Kurtikyan, T. S.; Hayrapetyan, V. A.; Martirosyan, G. G.; Ghazaryan, R. K.; Iretskii, A. V.; Zhao, H.; Pierloot, K.; Ford, P. C. *Chem. Commun.* **2012**, *48*, 12088−12090.
(56) (a) Goodrich, L. E.; Roy, S.; Alp, E. E.; Zhao, J.; Hu, M. Y.; Lehnert, N. *Inorg. Chem.* **2013**, *52*, 7766−7780. (b) Speelman, A. L.; Lehnert, N. *Acc. Chem. Res.* **2014**, *47*, 1106−1116.
(57) Merkle, A. C.; Fry, N. L.; Mascharak, P. K.; Lehnert, N. *Inorg. Chem.* **2011**, *50*, 12192−12203.
(58) Enemark, J.; Feltham, R. *Coord. Chem. Rev.* **1974**, *13*, 339−406.
(59) Zilberberg, I.; Ruzankin, S. P. *Chem. Phys. Lett.* **2004**, *394*, 165−170.
(60) Tomson, N. C.; Crimmin, M. R.; Petrenko, T.; Rosebrugh, L. E.; Sproules, S.; Boyd, W. C.; Bergman, R. G.; DeBeer, S.; Toste, F. D.; Wieghardt, K. *J. Am. Chem. Soc.* **2011**, *133*, 18785−18801.
(61) Remenyi, C.; Kaupp, M. *J. Am. Chem. Soc.* **2005**, *127*, 11399−11413.
(62) Pierloot, K.; Zhao, H.; Vancoillie, S. *Inorg. Chem.* **2010**, *49*, 10316−10329.
(63) Harvey, J. N. *Annu. Rep. Prog. Chem., Sect. C: Phys. Chem.* **2006**, *102*, 203−226.
(64) (a) Polo, V.; Gräfenstein, J.; Kraka, E.; Cremer, D. *Theor. Chem. Acc.* **2003**, *109*, 22−35. (b) Cremer, D.; Filatov, M.; Polo, V.; Kraka, E.; Shaik, S. *Int. J. Mol. Sci.* **2002**, *3*, 604−638. (c) Hughes, T. F.; Friesner, R. A. *J. Chem. Theory Comput.* **2011**, *7*, 19−32.
(65) When comparing computed harmonic frequencies with experimental fundamental transitions, one should also take into account a systematic error cancellation between the neglect of anharmonicity and inherent inaccuracy of the computed Hessian; see (a) Fouqueau, A.; Mer, S.; Casida, M. E.; Daku, L. M. L.; Hauser, A.; Mineva, T.; Neese, F. *J. Chem. Phys.* **2004**, *120*, 9473−9486. (b) Neese, F. *J. Biol. Inorg. Chem.* **2006**, *11*, 702−711.
(66) Madura, P.; Scheidt, W. R. *Inorg. Chem.* **1976**, *15*, 3182−3184.
(67) (a) Gonzalez, B.; Kouba, J.; Yee, S.; Reed, C. A.; Kirner, J. F.; Scheidt, W. R. *J. Am. Chem. Soc.* **1975**, *97*, 3247−3249. (b) Kirner, J. F.; Reed, C. A.; Scheidt, W. R. *J. Am. Chem. Soc.* **1977**, *99*, 1093−1101.
(68) Note that the Mn(TPP)(NO) has been recently reported[55] to have low-energy triplet state, which may be thermally populated at room temperature, although the ground state is singlet.
(69) Radoń, M. *Phys. Chem. Chem. Phys.* **2014**, *16*, 14479−14488.
(70) It is noteworthy that B3LYP gives $\Delta G_{migr} < 0$ only if spin-projected BS results are used for CoP(NO). For this reason, B3LYP data in ref 23 incorrectly indicate that $\Delta E_{Mn-NO}$ is greater than $\Delta E_{Co-NO}$ by as much as 7.5 kcal/mol. The present B3LYP data give at least the correct sign of $\Delta G_{migr}$, although both binding energies are clearly too low (cf. Figure 3), and BS B3LYP structural parameters of CoP(NO) are far from being perfect (cf. Table 1). Much better structural parameters and NO binding energies can be obtained from BS calculations with the B3LYP* and TPSSh functionals.
(71) The dissociation limit $^6$MnP + $^2$NO correspond to both (S = 2) and (S = 3) energy surfaces, which become degenerate for infinite Mn···NO distance. However, for any finite distance, the (S = 2) state will be lower in energy due to additional bonding stabilization.
(72) Poli, R.; Harvey, J. N. *Chem. Soc. Rev.* **2003**, *32*, 1−8.
(73) Shaik, S.; Chen, H.; Janardanan, D. *Nat. Chem.* **2011**, *3*, 19−27.
(74) Hoshino, M.; Kogure, M. *J. Phys. Chem.* **1989**, *93*, 5478−5484.
(75) At the time these kinetic studies were performed, the existence of a low-energy triplet isomer was unknown—likewise, its spectrum, needed to be determine the reaction rate from interpretation of time-resolved UV−vis spectroscopy (after laser flash photodenitrosylation). Note that the triplet and singlet isomers should have different spectral characteristics due to different MnNO geometries.
(76) (a) Swart, M. *Int. J. Quantum Chem.* **2013**, *113*, 2−7. (b) Ghosh, A. *J. Biol. Inorg. Chem.* **2006**, *11*, 712−724. (c) Harvey, J. N. *Struct. Bonding (Berlin, Ger.)* **2004**, *112*, 151−183.
(77) Ali, M. E.; Sanyal, B.; Oppeneer, P. M. *J. Phys. Chem. B* **2012**, *116*, 5849−5859.
(78) Jensen, K. P. *Inorg. Chem.* **2008**, *47*, 10357−10365.
(79) (a) Ganzenmüller, G.; Berkaïne, N.; Fouqueau, A.; Casida, M. E.; Reiher, M. *J. Chem. Phys.* **2005**, *122*, 234321. (b) Lawson Daku, L. M.; Aquilante, F.; Robinson, T. W.; Hauser, A. *J. Chem. Theory Comput.* **2012**, *8*, 4216−4231.
(80) Siegbahn, P. E. M. *J. Biol. Inorg. Chem.* **2006**, *11*, 695−701.
(81) Jaworska, M. *Chem. Phys.* **2007**, *332*, 203−210.
(82) Jiang, W.; DeYonker, N. J.; Wilson, A. K. *J. Chem. Theory Comput.* **2011**, *8*, 460−468.


DOI: 10.1021/ic503109a
*Inorg. Chem.* 2015, 54, 5634−5645